Immunity
Article

Unc93B1 Restricts Systemic Lethal Inflammation by Orchestrating Toll-like Receptor 7 and 9 Trafficking

Ryutaro Fukui,[1] Shin-Ichiroh Saitoh,[1] Atsuo Kanno,[1] Masahiro Onji,[1] Takuma Shibata,[1,2] Akihiko Ito,[4] Morikazu Onji,[5] Mitsuru Matsumoto,[6] Shizuo Akira,[7,8] Nobuaki Yoshida,[3] and Kensuke Miyake[1,2,*]
[1]Division of Infectious Genetics, Department of Microbiology and Immunology
[2]Laboratory of Innate Immunity
[3]Laboratory of Developmental Genetics, Center for Experimental Medicine and Systems Biology
The Institute of Medical Science, The University of Tokyo, 4-6-1 Shirokanedai, Minatoku, Tokyo 108-8639, Japan
[4]Department of Pathology, Faculty of Medicine, Kinki University, Osaka 589-8511, Japan
[5]Department of Gastroenterology and Metabology, Ehime University Graduate School of Medicine, Ehime 791-0295, Japan
[6]Division of Molecular Immunology, Institute for Enzyme Research, University of Tokushima, Tokushima 770-8504, Japan
[7]Laboratory of Host Defense, World Premier International Immunology Frontier Research Center, Osaka 565-0871, Japan
[8]Department of Host Defense, Research Institute for Microbial Diseases, Osaka University, Osaka 565-0871, Japan
*Correspondence: kmiyake@ims.u-tokyo.ac.jp
DOI 10.1016/j.immuni.2011.05.010

SUMMARY

Toll-like receptor-7 (TLR7) and 9, innate immune sensors for microbial RNA or DNA, have been implicated in autoimmunity. Upon activation, TLR7 and 9 are transported from the endoplasmic reticulum (ER) to endolysosomes for nucleic acid sensing by an ER-resident protein, Unc93B1. Little is known, however, about a role for sensor transportation in controlling autoimmunity. TLR9 competes with TLR7 for Unc93B1-dependent trafficking and predominates over TLR7. TLR9 skewing is actively maintained by Unc93B1 and reversed to TLR7 if Unc93B1 loses preferential binding via a D34A mutation. We here demonstrate that mice harboring a D34A mutation showed TLR7-dependent, systemic lethal inflammation. CD4$^+$ T cells showed marked differentiation toward T helper 1 (Th1) or Th17 cell subsets. B cell depletion abolished T cell differentiation and systemic inflammation. Thus, Unc93B1 controls homeostatic TLR7 activation by balancing TLR9 to TLR7 trafficking.

INTRODUCTION

Toll-like receptors (TLRs) sense a variety of microbial products such as microbial membrane lipids or nucleic acids and mount innate and adaptive immune responses (Kaisho and Akira, 2006; Miyake, 2007). Cell-surface TLR dimers including TLR4-MD-2, TLR1-TLR2, and TLR6-TLR2 recognize microbial membrane lipids, whereas TLR3, 7, 8, and 9 reside in intracellular organelles and recognize microbial nucleic acids. Recent studies have revealed that TLRs mistakenly respond to self products and cause autoimmune diseases. TLR7 and 9, innate immune sensors for microbial RNA or DNA (Blasius and Beutler, 2010), have been implicated in autoimmune diseases such as psoriasis (Lande et al., 2007), arthritis (Asagiri et al., 2008), and systemic lupus erythematosus (SLE) (Christensen et al., 2006; Ehlers et al., 2006; Marshak-Rothstein and Rifkin, 2007). Overexpression of TLR7 in the Y-linked autoimmune accelerating (Yaa) mice or TLR7 transgenic mice predisposes these organisms to lupus nephritis (Deane et al., 2007; Subramanian et al., 2006), whereas the lack of the TLR7 gene ameliorates disease progression in lupus-prone mice (Christensen et al., 2006). TLR9 is more complicated than TLR7 in its link with autoimmune disease. Despite reports showing a pathogenic role for TLR9 in psoriasis, lupus nephritis, adjuvant-induced arthritis, or a mouse model of multiple sclerosis (Asagiri et al., 2008; Deng et al., 1999; Ehlers et al., 2006; Ronaghy et al., 2002), opposing results were also described that TLR9 deficiency in autoimmune-prone MRL/lpr mice exacerbates clinical diseases, including more severe glomerulonephritis, a significantly shortened lifespan, and in some models, elevated titers of autoantibodies reactive with RNA-associated autoantigens (Christensen et al., 2006; Yu et al., 2006). TLR9 was suggested to protect disease progression by antagonizing TLR7 (Nickerson et al., 2010). An opposing relationship between TLR7 and 9 has emerged as a potential mechanism regulating autoimmunity.

Self-pathogen discrimination by TLR7 and 9 was initially considered to depend on structural differences between self and microbial nucleic acids, such as unmethylated CpG motifs in bacterial DNA and clusters of U- or GU-rich sequences in viral RNA (Diebold et al., 2004; Heil et al., 2004; Krieg, 2002). However, these structures recognized by TLR7 and 9 are still found in self nucleic acids, although much less than in microbial nucleic acids. Therefore, TLR7 and 9 still have the risk of responding to self nucleic acids. Self-pathogen discrimination needs to be strengthened by sequestration of self nucleic acids from endolysosomes, the site for nucleic acid sensing by TLR7 and 9. Whereas extracellular self nucleic acids are rapidly degraded by DNase or RNase, microbial nucleic acids are protected by bacterial cell walls or viral particles and transported to endolysosome (Barton et al., 2006). Aberrant trafficking of self nucleic acids to endolysosomes was shown to exacerbate autoimmunity (Lande et al., 2007; Leadbetter et al., 2002; Marshak-Rothstein and Rifkin, 2007). In autoimmune diseases like SLE, self-RNA and self-DNA are complexed with autoantibodies against the nucleic acid or nucleoproteins, delivered

into endosomal compartments via FcγRII-mediated endocytosis, leading to dendritic cell (DC) activation and production of type I interferon (IFN) (Barrat et al., 2005). In psoriasis, self-DNA and -RNA form complexes with the cationic antimicrobial peptide LL37, gain access to TLR7 and 9 in endolysosomes of DCs, and induce aberrant production of IFN-α (Ganguly et al., 2009; Lande et al., 2007).

TLR7 and 9 are also transported from the endoplasmic reticulum (ER) to endolysosomes upon activation. TLR7 and 9 trafficking is controlled by Unc93B1, a multitransmembrane ER-resident protein. In mice, a missense mutation in the *Unc93b1* gene (H412R mutation) abrogates signaling via TLR3, 7, and 9 without compromising other TLRs (Tabeta et al., 2006). These mutant mice ("3d" mice) show increased susceptibility to infection by a variety of pathogens. As in 3d mice, cells from Unc93B1-deficient patients are defective in signaling via the nucleic acid-sensing TLRs 3, 7, 8, and 9 (Casrouge et al., 2006). Unc93B1 was shown to bind to TLR7 and 9 and transport TLR7 and 9 from the ER to endolysosomes (Brinkmann et al., 2007; Kim et al., 2008). The 3d mutation H412R of Unc93B1 abolishes these interactions. Unc93B1-dependent trafficking of TLR7 and 9 might have a role in limiting excessive access of TLR7 and 9 to their ligands in endolysosome.

We previously reported that TLR9 competes with TLR7 for Unc93B1-dependent transportation and predominates over TLR7 (Fukui et al., 2009). TLR9 predominance is reversed to TLR7 by D34A mutation in Unc93B1, rendering TLR7 hyperresponsive and TLR9 hyporesponsive in dendritic cells (Fukui et al., 2009). Mice harboring a D34A mutation in Unc93B1 have now been established and we here show a critical role for Unc93B1 in restricting homeostatic TLR7 activation.

RESULTS

A D34A Mutation in Unc93B1 Skews the TLR7 and TLR9 Balance to TLR7

To address a role for Unc93B1-dependent TLR7 and 9 balance in vivo, we generated the mice harboring a single base mutation replacing D34 with A in Unc93B1 by gene targeting (see Figures S1A and S1B available online). Homozygous mice were born at the expected Mendelian ratio without any obvious developmental defect (Figure S1C). The mutation was confirmed by sequencing genomic DNA from *Unc93b1*$^{D34A/D34A}$ homozygous mice (Figure S1D).

We previously reported that overexpression of a D34A Unc93B1 mutant rendered TLR7 hyperresponsive and TLR9 hyporesponsive in bone marrow-derived conventional dendritic cells (BM-cDCs) (Fukui et al., 2009). To confirm and extend this finding by using *Unc93b1*$^{D34A/D34A}$ mice, we obtained BM-Mac (macrophage), BM-cDCs, BM-pDCs (plasmacytoid DC), and B cells from *Unc93b1*$^{D34A/D34A}$ mice, and we stimulated them with TLR7 ligands (loxoribine or imiquimod), TLR9 ligands (CpG-A or CpG-B), a TLR3 ligand (poly(I:C)), or a TLR4-MD-2 ligand (lipid A). Production of tumor necrosis factor-α (TNF-α), interleukin-12 (IL-12) p40, or IFN-α was detected by ELISA (Figures 1A–1C). B cells were cultured with TLR ligands and proliferation was estimated by ^{3}H-labeled thymidine uptake assay (Figure 1D). As expected, the TLR7 response was upregulated whereas the TLR9 response was downregulated in all the immune cells studied from *Unc93b1*$^{D34A/D34A}$ mice (Figures 1A–1D). TLR3 and TLR4-MD-2 responses were not affected by the D34A mutation (Figures 1A, 1B, and 1D). Despite these TLR7-skewed responses in these immune cells, the D34A mutation did not alter mRNA expression encoding TLR7 or TLR9 (Figure 1E; Figures S2A and S2B). These results demonstrate that Unc93B1 actively maintains the TLR9-skewed state in these immune cells.

Systemic Lethal Inflammation in *Unc93b1*$^{D34A/D34A}$ Mice

Half of the *Unc93b1*$^{D34A/D34A}$ mice prematurely died within 30 weeks of age (Figure 2A). Huge splenomegaly and liver damage were macroscopically apparent in moribund mice. Pale spots on the entire surface of the liver were macroscopically seen, suggesting multilobular liver damages. Microscopic analyses with H&E staining of moribund mice revealed multilobular hepatic necrosis (Figure 2B, green arrowheads) probably caused by ischemia and infiltration of inflammatory cells into the hepatic sinusoids and slightly into the portal area (black arrowheads). These pathological findings suggested acute huge liver damage, which probably induced liver failure. Flow cytometry analyses revealed that CD11b^{+} CD11c^{hi}Gr1^{int} cells infiltrated the liver (Figure 2C). Although the reticulin fiber was partly aggregated in silver impregnation stain (Figure 2B, open arrowheads), progressive portal fibrosis, indicating chronic liver damage, was not clearly observed. Elevated amounts of serum bilirubin, AST (aspartate aminotransferase), and ALT (alanine aminotransferase) corroborated hepatic necrosis in moribund mice (Figure 2D; Figure S3A). In nonmoribund mice, liver specimens indicated only mild to moderate infiltration of inflammatory cells into sinusoids and spotty hepatic necrosis mainly in the central area of the liver lobule (Figure 2B, blue arrowheads), suggesting that the liver damage was not severe. Consistent with this, serum AST and ALT were not elevated in nonmoribund mice (Figure S3A). Necrotic lesions were not found in other organs including kidney, lung, heart, and spleen (Figures 2E and 3B; Figure S3C). In the kidney, glomerulonephritis was microscopically apparent (Figure 2E), but the function of kidneys seemed to be spared, because serum creatinine showed only a weak increase (Figure 2F; Figure S3A). Premature death in *Unc93b1*$^{D34A/D34A}$ mice is, therefore, likely to be caused by liver necrosis rather than glomerulonephritis (see Discussion).

Splenomegaly was progressive and correlated well with mouse mortality (Figure 3A). Histological analyses demonstrated that the tissue structure of the spleen was disrupted by massive expansion of nonlymphoid cells (Figure 3B). Flow cytometry analyses revealed that Ter119^{+}CD71^{+} erythroblasts and CD11b^{+} myeloid cells increased in the spleen at the cost of T cells (Figure 3C). CD11b^{+} myeloid cells in the spleen were likely to migrate through the portal vein into the liver and caused hepatocyte necrosis. Expansion of erythroid and myeloid cells did not change the percentage of B cells (Figure 3C), suggesting that B cells also increased in number. Despite erythroblastosis in the spleen, anemia was seen only in moribund mice (Figure S3B). Instead, a blood cell count revealed severe thrombocytopenia not only in moribund mice but also in nonmoribund mice (Figure 3D).

We also examined autoantibody production by histological staining. We were able to detect antinuclear (ANA), mitochondorial (AMA), and smooth muscle antibodies (ASMA) (Figure S3D) in *Unc93b1*$^{D34A/D34A}$ mice.

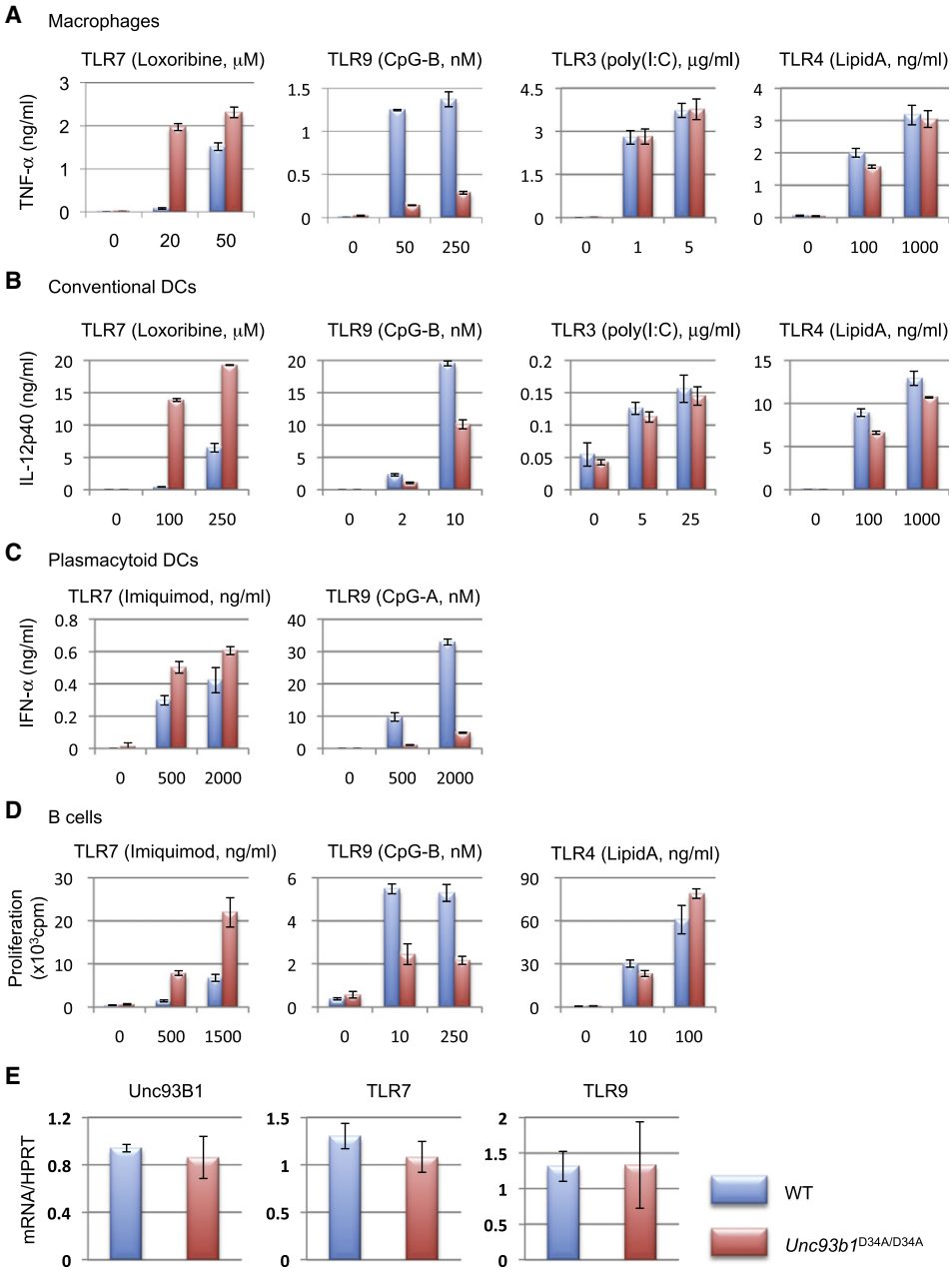

Figure 1. A D34A Mutation in Unc93B1 Renders TLR7 Hyperresponsive and TLR9 Hyporesponsive

(A–C) Cytokine production of bone marrow-derived macrophages (A), cDCs (B), or pDCs (C). TNF-α (A), IL-12p40 (B), or IFN-α (C) in culture supernatant were detected by ELISA.

(D) Proliferation assay of splenic B cells. B cell proliferation was detected by ^{3}H-labeled thymidine uptake after 3 days of stimulation.

(E) mRNA expression in bone marrow-derived macrophages. Results were normalized by HPRT mRNA expression.

Blue bars or red bars indicate cells from *Unc93b1*$^{WT/WT}$ mice or *Unc93b1*$^{D34A/D34A}$ mice, respectively. Cells were stimulated with TLR7 (loxoribine, μM; Imiquimod, ng/ml), TLR9 (CpGA or CpG-B, nM), TLR3 (poly(I:C), μg/ml), or TLR4 (LipidA, ng/ml) ligands (A)–(D). Mean ± SD from triplicate wells. Representative results are shown from at least three independent analyses with mice at 5–10 weeks old. See also Figure S2.

TLR7, but Not TLR9, Is Responsible for the Pathologies in *Unc93b1*$^{D34A/D34A}$ Mice

To clarify roles for TLR7 or 9 in the pathologies of *Unc93b1*$^{D34A/D34A}$ mice, we crossed *Unc93b1*$^{D34A/D34A}$ mice with *Myd88*$^{-/-}$, *Tlr7*$^{-/-}$, or *Tlr9*$^{-/-}$ mice. *Unc93b1*$^{D34A/D34A}$ *Tlr7*$^{-/-}$ mice did not show premature death, whereas the lack of TLR9 did not alter survival of *Unc93b1*$^{D34A/D34A}$ mice (Figure 4A). Furthermore, aberrant expansion of erythroblast and myeloid cells was not seen in the spleen of *Unc93b1*$^{D34A/D34A}$ *Tlr7*$^{-/-}$ mice (Figure 4B). Platelet counts in peripheral blood returned to normal in the absence of MyD88 or TLR7, but not of TLR9 (Figure 4C).

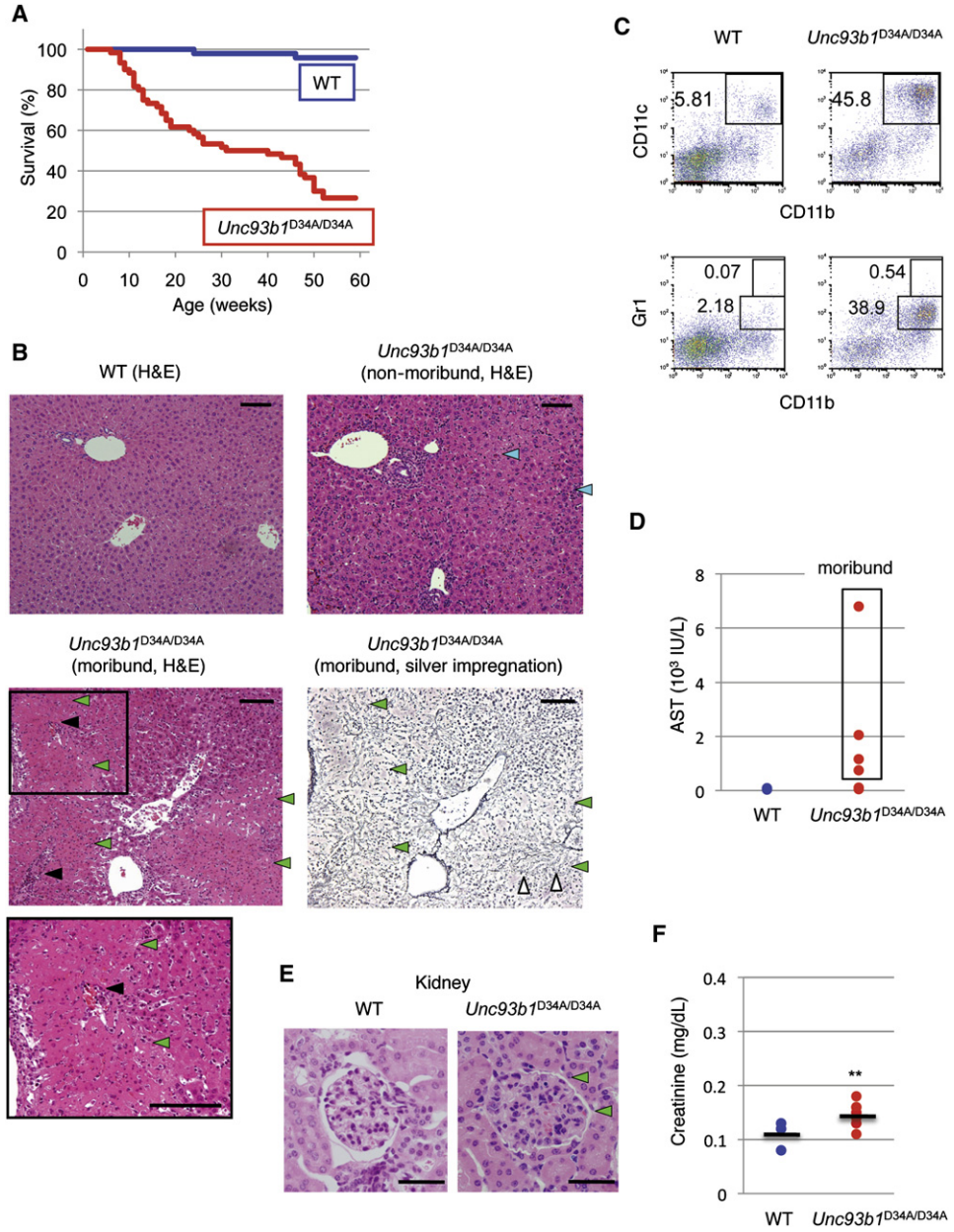

Figure 2. The D34A Unc93B1 Mutation Causes Systemic Inflammation

(A) Survival curves for wild-type mice (blue, n = 48) and *Unc93b1*$^{D34A/D34A}$ mice (red, n = 60).

(B) Histological (hematoxyline and eosine, H&E, or silver impregnation) analyses of the liver. The left bottom photo shows the area indicated by a square in the left middle photo. Left middle and right middle photos were serially prepared. Green arrowheads, the boundary of multilobular necrotic areas; black arrowheads, inflammatory cell infiltration; open arrowheads, aggregation of reticulin fiber in the necrotic area; blue arrowheads, spotty hepatic necrosis. Scale bars represent 100 μm.

(C) Flow cytometry analyses of liver cells.

(D) Serum AST scores. The data points indicated by a square are values for moribund mice.

(E) Histological analyses of kidneys. The arrowheads indicate the boundary of a glomerulus. Scale bars represent 100 μm.

(F) Creatinine in peripheral blood from wild-type or *Unc93b1*$^{D34A/D34A}$ mice.

Blue dots or red dots in (D) and (F) indicate WT (n = 6) or *Unc93b1*$^{D34A/D34A}$ (n = 9) mice, respectively. Statistics analysis was calculated by Student's t test. **p < 0.001. Data are representative of at least six independent analyses of mice at 17–37 weeks old. See also Figure S3.

We next studied subcellular distribution of TLR7 or TLR9 in DCs. GFP-tagged TLR7 or TLR9 was expressed in stem cell-transduced DCs, and the distribution of TLR7 or TLR9 was determined by confocal microscopy (Figure 4D; Figure S7). TLR7-GFP in *Unc93b1*$^{D34A/D34A}$ DCs showed higher colocalization with an endolysosome marker LAMP1 than that in wild-type DCs. The percentage of the cells showing TLR7-LAMP1 colocalization in *Unc93b1*$^{D34A/D34A}$ DCs was about 2-fold higher than that in

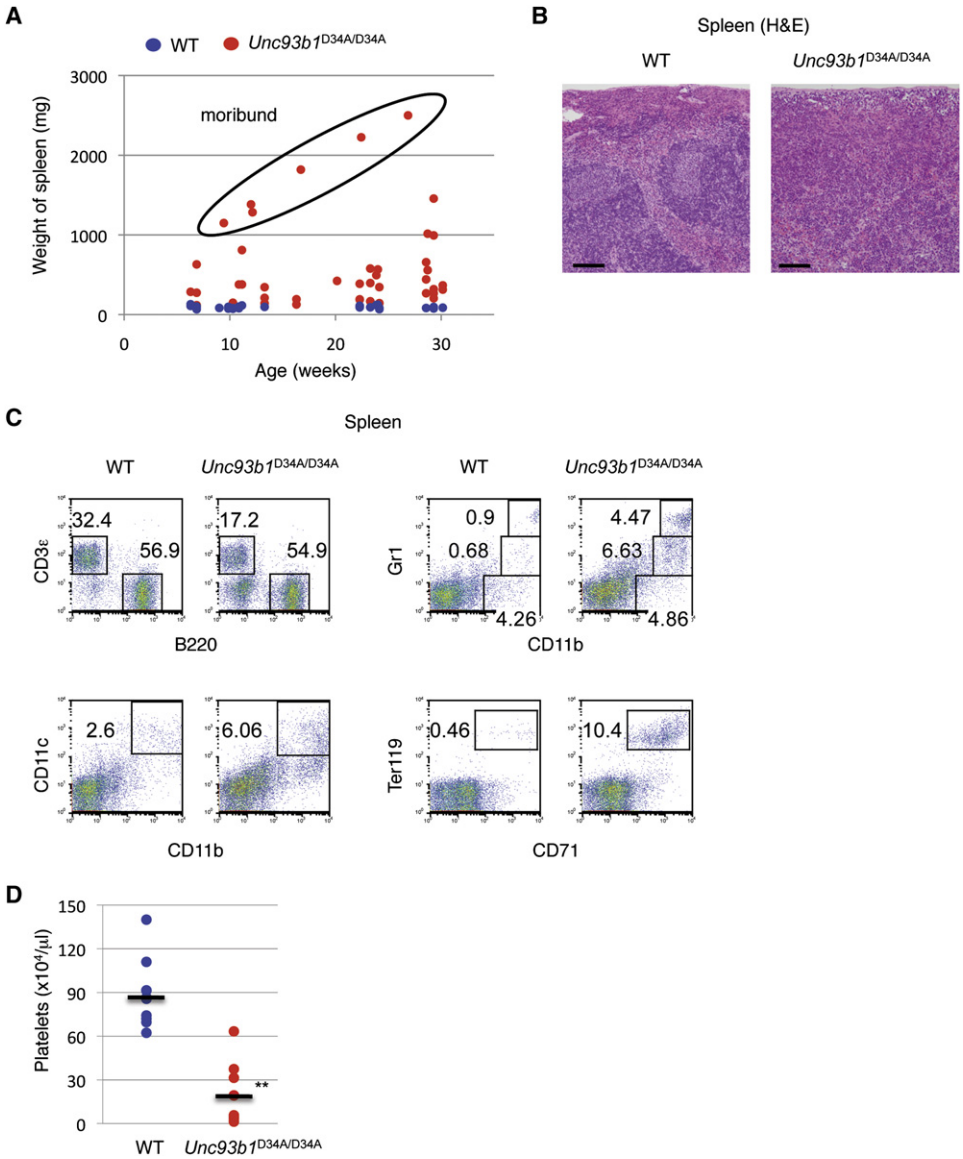

Figure 3. Pathologic Changes in *Unc93b1*$^{D34A/D34A}$ Mice

(A) Plot of spleen weight against ages of the mice. The values from moribund mice are indicated by an ellipse.

(B) Microscopic analyses of the spleen. Histological samples were stained by H&E. Scale bars represent 100 μm.

(C) Flow cytometry analyses of splenic cells.

(D) Platelet counts in peripheral blood from wild-type (n = 9) or *Unc93b1*$^{D34A/D34A}$ mice (n = 12). Black bars in the graph indicate the averages (WT = 88.1, KI = 19.8). Blue dots or red dots in (A) and (D) indicate WT or *Unc93b1*$^{D34A/D34A}$ mice, respectively. Statistics analysis was calculated by Student's t test. **$p < 0.001$. Data are representative of at least six independent analyses of mice at 18–37 weeks old. See also Figure S3.

wild-type DCs (Figure 4E). In contrast, no difference was seen between *Unc93b1*$^{D34A/D34A}$ and wild-type DCs in colocalization of TLR9-GFP and LAMP-1 (Figure S7). These results suggest that aberrant activation of TLR7 in *Unc93b1*$^{D34A/D34A}$ mice results from enhanced TLR7 trafficking to endolysosomes.

T Cells Show Marked Differentiation into Th1 or Th17 Cell Subsets in *Unc93b1*$^{D34A/D34A}$ Mice

To gain insight into the pathology of *Unc93b1*$^{D34A/D34A}$ mice, we studied the activation status of T cells. CD4$^+$ T cells showed marked differentiation toward a CD62L^{lo}CD44^{hi} memory phenotype (Figure 5A). Cell surface ICOS (inducible T cell costimulator) and CD69 were both upregulated in lymph node CD4$^+$ T cells (Figure 5B). The lack of TLR7 completely abolished these changes (Figures 5A and 5B), suggesting that chronic T cell activation is linked to TLR7-dependent pathology in *Unc93b1*$^{D34A/D34A}$ mice. To corroborate a pathogenic role for lymphocytes in the pathology of *Unc93b1*$^{D34A/D34A}$ mice, *Unc93b1*$^{D34A/D34A}$ mice were crossed with *Rag2*$^{-/-}$ mice. The double mutant mice did not suffer from premature death, splenomegaly, or thrombocytopenia (Figures 5C and 5D), demonstrating a key role for lymphocytes in systemic inflammation caused by the D34A mutation.

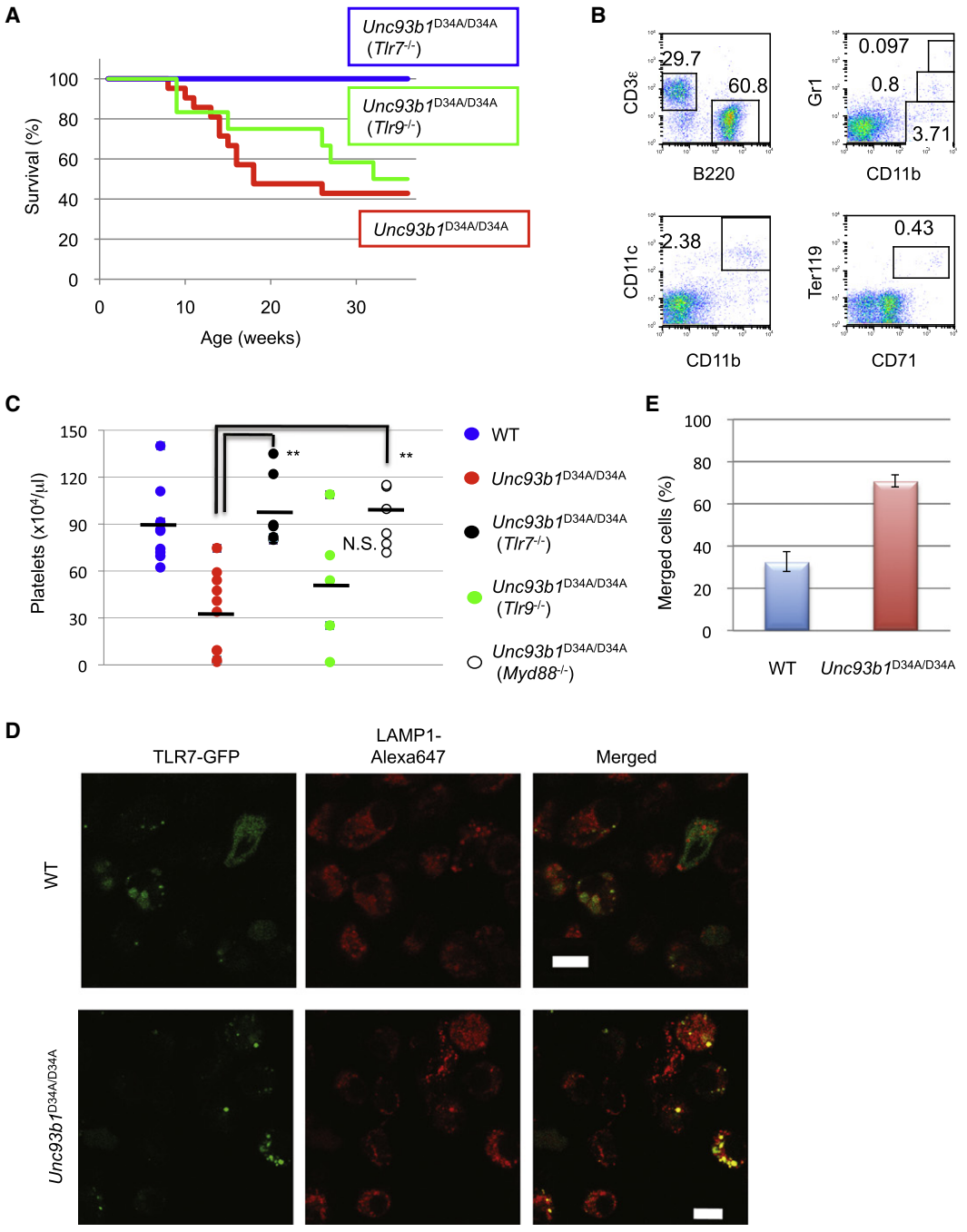

Figure 4. TLR7 Causes Systemic Inflammation in *Unc93b1*$^{D34A/D34A}$ Mice

(A) Survival curves of *Unc93b1*$^{D34A/D34A}$ mice (red, n = 21) or those lacking TLR7 (blue, n = 15) or TLR9 (green, n = 12).

(B) Flow cytometry analyses of splenic cells from *Unc93b1*$^{D34A/D34A}$*Tlr7*$^{-/-}$ mice.

(C) Platelet counts in peripheral blood from mice of the indicated genotypes.

(D) Intracellular distribution of TLR7 in stem cell-derived DCs. LAMP1 was used as a marker of endolysosomes. Scale bars represent 10 μm.

(E) Percentage of the cells in which TLR7 are merged with endolysosomes. More than 30 cells were observed and calculated.

Statistics analyses were calculated by Student's t test between indicated genotype. **p < 0.001, N.S., not significant. Data are representative of at least five independent analyses of mice at 17–40 weeks old. See also Figure S7.

ICOS upregulation on CD4$^+$ T cells in *Unc93b1*$^{D34A/D34A}$ mice correlated with spleen weight (Figure S4). ICOS was reported to be important for the development of follicular helper T (Tfh) cells or IL-17A-producing helper T (Th17) cells (Bauquet et al., 2009). To study the in vivo activation status of helper T cell subsets in *Unc93b1*$^{D34A/D34A}$ mice, cytokine expression in CD4$^+$

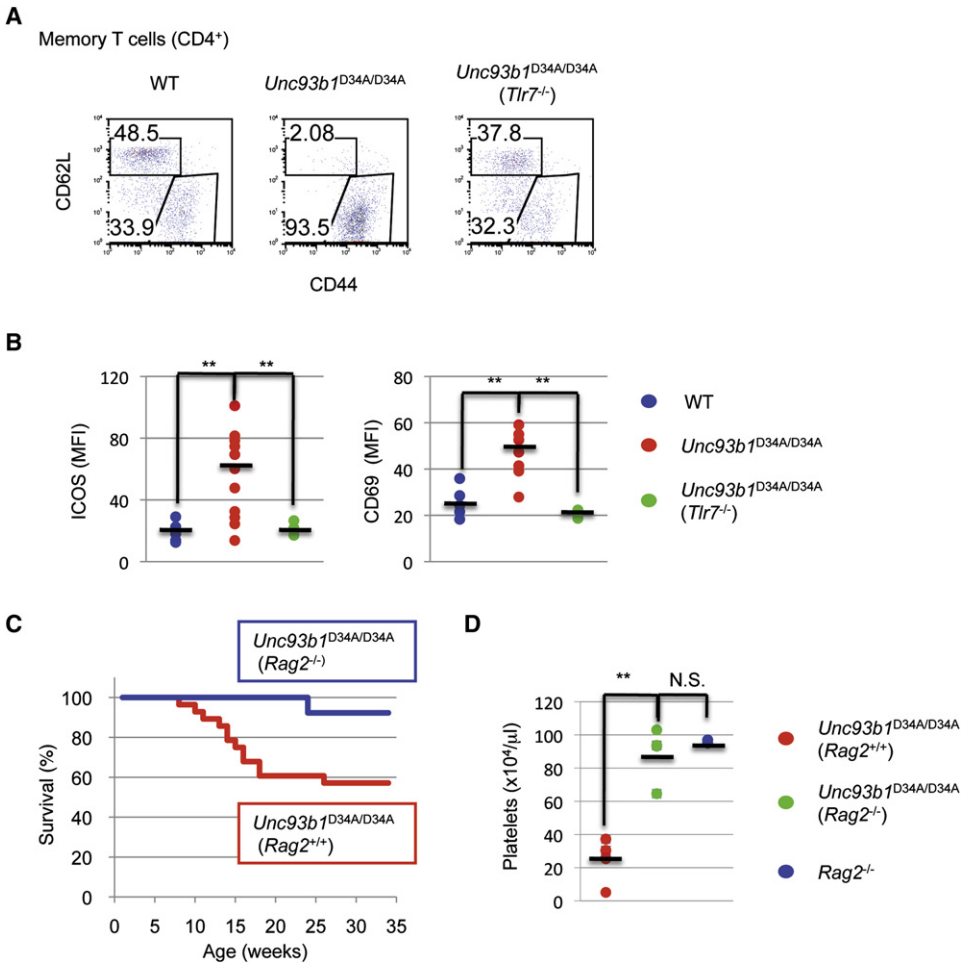

Figure 5. Lymphocytes Are Responsible for Systemic Inflammation in *Unc93b1*$^{D34A/D34A}$ Mice

(A) Flow cytometry analyses of CD4$^+$ T cells from WT, *Unc93b1*$^{D34A/D34A}$, or *Unc93b1*$^{D34A/D34A}$*Tlr7*$^{-/-}$ mice for memory T cells (CD44^{hi}CD62L^{lo}).

(B) Mean fluorescence intensities (MFI) of ICOS or CD69 on CD4$^+$ T cells from wild-type (blue), *Unc93b1*$^{D34A/D34A}$ (red), or *Unc93b1*$^{D34A/D34A}$*Tlr7*$^{-/-}$ (green) mice. Black bars represent average values.

(C) Survival curves of *Unc93b1*$^{D34A/D34A}$ (red, n = 28) or *Unc93b1*$^{D34A/D34A}$*Rag2*$^{-/-}$ (blue, n = 13) mice.

(D) Platelet counts in peripheral blood from WT (red), *Unc93b1*$^{D34A/D34A}$*Rag2*$^{-/-}$ (green), or *Rag2*$^{-/-}$ (blue) mice. Black bars represent average values (24.8, 89.5, 96.0, respectively).

Statistics analyses were calculated by Student's t test between indicated genotype. **p < 0.001. N.S., not significant. Data are representative of at least five independent analyses of mice at 18–37 weeks old. See also Figure S4.

T cells was analyzed and compared between wild-type and *Unc93b1*$^{D34A/D34A}$ mice. mRNA encoding IL-17A or IFN-γ was upregulated, suggesting enhanced T cell differentiation into Th17 and Th1 cells (Figure 6A). Th17 cell differentiation was further supported by upregulation of the mRNA for another Th17 cell-specific cytokine IL-22 (Figure 6A). To confirm enhanced T cell differentiation into Th1 and Th17 cells, percentages of Th1 and Th17 cells were determined by intracellular staining of IL-17A and IFN-γ. As expected, Th1 and Th17 cells increased in percentage in lymph nodes from *Unc93b1*$^{D34A/D34A}$ mice in a manner dependent on TLR7 (Figure 6B). IL-21 is produced in Tfh and Th17 cells and has a pathogenic role in BXSB-Yaa mice (Bubier et al., 2009), an autoimmune-prone mouse resulting from TLR7 gene duplication (Pisitkun et al., 2006; Subramanian et al., 2006). mRNA encoding IL-21 as well as the chemokine Ccl5 (RANTES), was upregulated in *Unc93b1*$^{D34A/D34A}$ mice. IFN-γ produced in CD8$^+$ T cells is reported to activate macrophages and cause hemophagocytic syndrome (Jordan et al., 2004). CD8$^+$ T cells in *Unc93b1*$^{D34A/D34A}$ mice also showed aberrant production of IFN-γ and Ccl5 (RANTES) (Figure S5A). Meanwhile, hemophagocytosis in the bone marrow and peripheral blood was also found (Figure S5B).

Pathogenic Roles for B Cells in *Unc93b1*$^{D34A/D34A}$ Mice

We finally examined a role for B cells in the pathology of *Unc93b1*$^{D34A/D34A}$ mice, by crossing these mice with B cell-deficient *Ighm*$^{-/-}$ mice (Kitamura et al., 1991). The double mutant mice did not show premature death or splenomegaly (Figure 7A). Interestingly, blood platelet count in *Unc93b1*$^{D34A/D34A}$*Ighm*$^{-/-}$ mice was significantly higher than that in *Unc93b1*$^{D34A/D34A}$ mice but was still lower than in wild-type mice (Figure 7B). In contrast, thrombocytopenia was not seen in *Unc93b1*$^{D34A/D34A}$

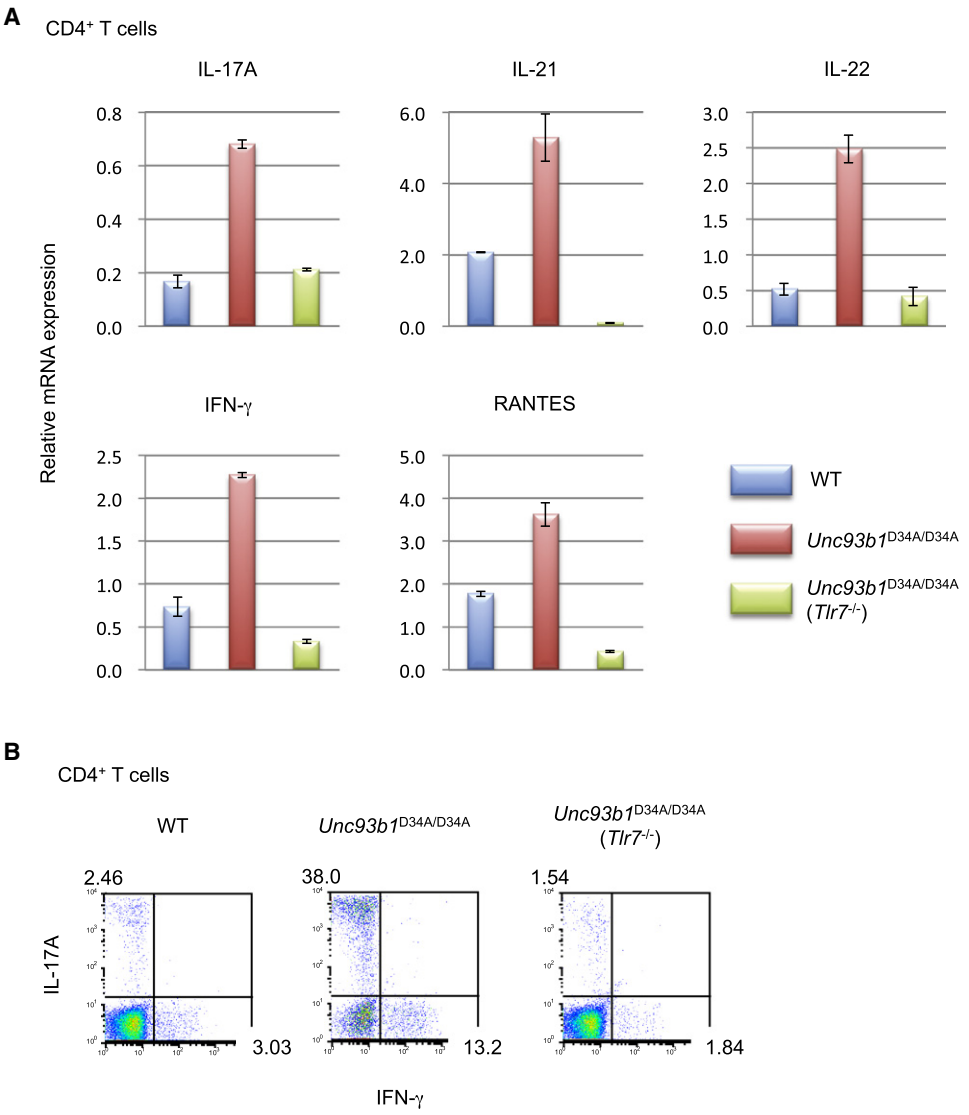

Figure 6. T Cells Show Marked Differentiation into Th1 or Th17 Cell Subsets in *Unc93b1*$^{D34A/D34A}$ Mice

(A) Real-time RT-PCR for indicated gene expression. CD4$^+$ T cells were obtained from wild-type (blue), *Unc93b1*$^{D34A/D34A}$ (red), or *Unc93b1*$^{D34A/D34A}$*Tlr7*$^{-/-}$ (green) mice. The results were normalized by HPRT mRNA and represented as mean values from triplicate wells.

(B) Intracellular IL-17A and IFN-γ in CD4$^+$ T cells. Lymph node T cells were stained after 5 hr stimulation of PMA and ionomycin.

Data are representative of at least five independent analyses of mice at 24–31 weeks old. See also Figure S5.

Rag2$^{-/-}$ mice (Figure 5D), suggesting that a T cell-dependent, B cell-independent mechanism caused mild thrombocytopenia. T cell-dependent activation of macrophages, probably through cytokines such as IFN-γ, likely enhanced aberrant platelet ingestion. B cells probably exacerbated thrombocytopenia by producing antiplatelet autoantibody or by enhancing T cell-dependent macrophage activation. B cells were required for robust T cell activation and differentiation in *Unc93b1*$^{D34A/D34A}$ mice. Differentiation toward CD62L^{lo}CD44^{hi} memory phenotypes and ICOS upregulation were not seen in CD4$^+$ T cells from *Unc93b1*$^{D34A/D34A}$*Ighm*$^{-/-}$ mice (Figures 7C and 7D).

Given the pathogenic roles for B cells, we examined the activation status of B cells in *Unc93b1*$^{D34A/D34A}$ mice. Serum IgG2a and IgG2b in unperturbed *Unc93b1*$^{D34A/D34A}$ mice were higher than those in wild-type mice (Figure 7E). In lymph nodes, B cells apparently increased in percentage (Figure 7F; Figure S6A). In the spleen, CD21^{hi}CD23$^-$ marginal zone B cells were reduced in percentage (Figure S6B). Alteration in B cell maturation and expansion was not found in *Unc93b1*$^{D34A/D34A}$*Tlr7*$^{-/-}$ mice (Figure 7F; Figure S6B). *Unc93b1*$^{D34A/D34A}$ B cells showed higher proliferation than wild-type B cells in response to anti-IgM as well as to TLR7 ligand (Figures 1D and 7G). These data suggest that TLR7 in B cells are constitutively activated in *Unc93b1*$^{D34A/D34A}$ mice.

DISCUSSION

Pathogenic roles for TLR7 in autoimmunity have been well documented. The Y-linked autoimmune accelerating (Yaa) locus is

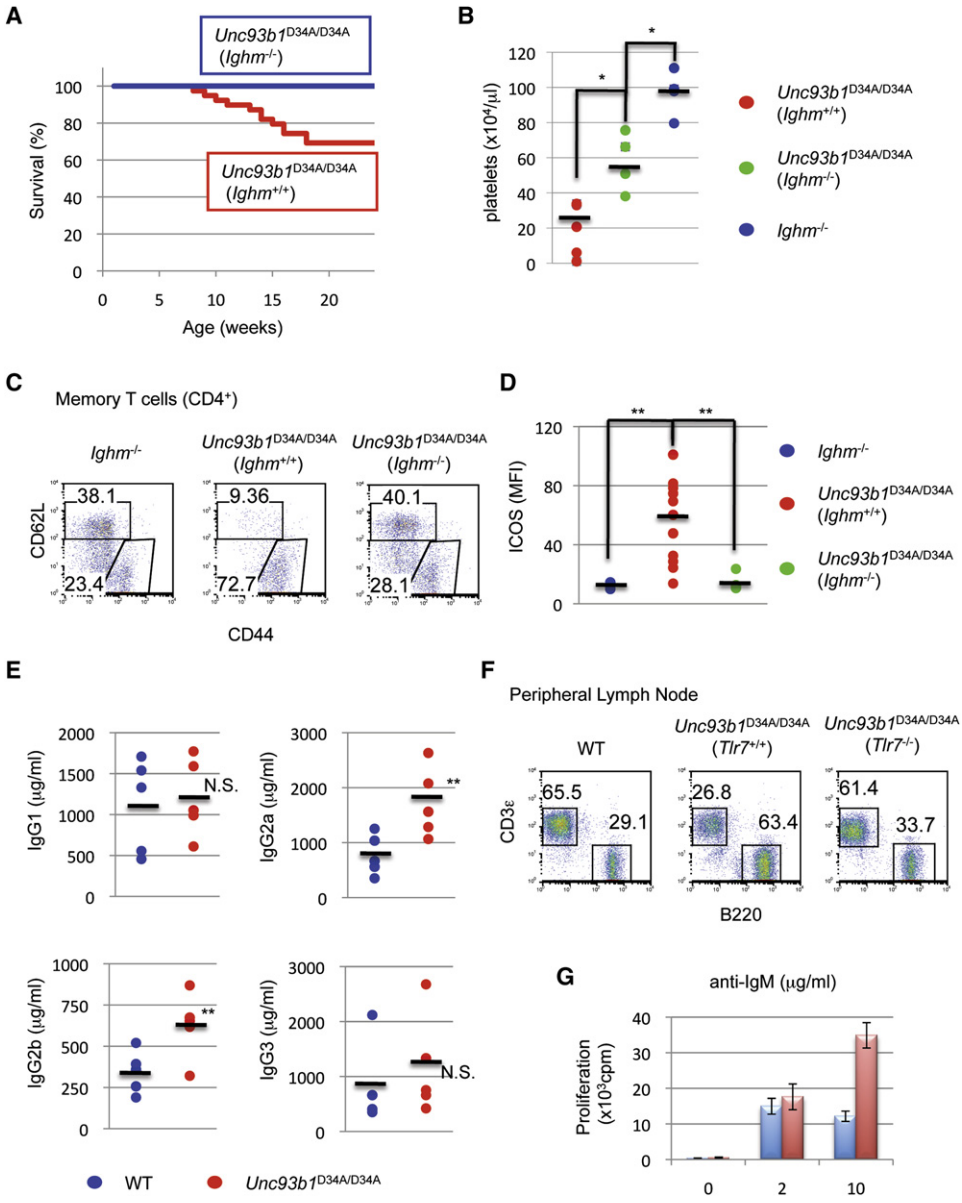

Figure 7. Pathogenic Roles for B Cells in *Unc93b1*$^{D34A/D34A}$ Mice

(A) Survival curves of *Unc93b1*$^{D34A/D34A}$ (red, n = 39) or *Unc93b1*$^{D34A/D34A}$*Ighm*$^{-/-}$ (blue, n = 16) mice.

(B) Platelet counts in peripheral blood from indicated mice.

(C) Flow cytometry analyses for memory phenotypes (CD44^{hi}CD62L^{lo}) of CD4^{+} T cells from *Ighm*$^{-/-}$, *Unc93b1*$^{D34A/D34A}$, and *Unc93b1*$^{D34A/D34A}$*Ighm*$^{-/-}$ mice.

(D) ICOS expression on CD4 T cells from *Ighm*$^{-/-}$ (blue), *Unc93b1*$^{D34A/D34A}$ (red), and *Unc93b1*$^{D34A/D34A}$*Ighm*$^{-/-}$ (green) mice. Black bars represent average values of MFI (12.2, 57.2, 14.5, respectively).

(E) Serum titers of IgG subclass.

(F) Flow cytometry showing T and B cells in lymph nodes from WT, *Unc93b1*$^{D34A/D34A}$, or *Unc93b1*$^{D34A/D34A}$*Tlr7*$^{-/-}$ mice. Percentages are shown.

(G) B cell proliferation in response to anti-IgM (μg/ml). Mean ± SD from triplicate wells.

Statistics analyses were calculated by Student's t test between indicated genotype. **p < 0.001, *p < 0.01, N.S., not significant. Data are representative of at least five independent analyses of mice at 17–37 weeks old. See also Figure S6.

a potent autoimmune disease allele because of TLR7 gene duplication (Pisitkun et al., 2006; Subramanian et al., 2006). Transgenic mice overexpressing TLR7 also causes autoimmunity (Deane et al., 2007). Despite the similarities between *Unc93b1*$^{D34A/D34A}$ and Yaa mice in the phenotypes like splenomegaly, glomerulonephritis, or monocytosis, apparent differences were also found. First, Th17 cell differentiation was enhanced in *Unc93b1*$^{D34A/D34A}$ mice but not in Yaa mice (Bubier et al., 2009). Second, liver necrosis was found in *Unc93b1*$^{D34A/D34A}$ mice but has never been reported in Yaa mice. Third, thrombocytopenia was not reported in Yaa mice, but in *Unc93b1*$^{D34A/D34A}$ mice. A link between TLR7 and Th17

cells has been previously reported. Strong activation of TLR7 in pDCs was suggested to promote T cell differentiation into Th17 or Th1 cells (Rajagopal et al., 2010; Yu et al., 2010). Topical application of a TLR7 agonist induces Th17 cell-dependent psoriasis-like skin inflammation and splenomegaly in mice (van der Fits et al., 2009). Strong TLR7 activation in pDCs and/or B cells may be required for T cell differentiation into Th17 or Th1 cell subsets. Thrombocytopenia may also depend on strong TLR7 activation, as indicated by the fact that thrombocytopenia was seen in TLR7 transgenic mice expressing as many as 8–16 copies of the TLR7 gene but not in those expressing 4–8 copies (Deane et al., 2007). Although mRNA for TLR7 was not altered by the D34A mutation, D34A mutation in Unc93B1 seems to be as pathogenic as 8–16 extra copies of the TLR7 gene, far beyond the TLR7 gene duplication. Robust TLR7 responses in *Unc93b1*$^{D34A/D34A}$ mice would be important for inducing Th17 and Th1 cell differentiation as well as massive monocytosis. On the other hand, weaker TLR7 activation in Yaa mice may predispose to a SLE-like autoimmune disease. This study provided in vivo evidence demonstrating that nucleic acid-sensor trafficking is controlled as much as nucleic acid trafficking to avoid innate immune response to self-nucleic acids.

TLR9 ameliorates disease progression in autoimmune-prone MRL/lpr mice (Christensen et al., 2006), and the protective role for TLR9 depends on its antagonistic effect on TLR7 (Nickerson et al., 2010). The signaling pathway downstream of TLR9 is indistinguishable from that of TLR7, so TLR9 is unlikely to deliver a unique signal antagonizing TLR7-dependent autoimmunity. Our studies strongly suggest that the antagonistic effect of TLR9 is mediated by its competition with TLR7 for interaction with Unc93B1 (Fukui et al., 2009). TLR8 has a similar role in regulating autoimmunity through its antagonistic effect on TLR7, as shown by the fact that *Tlr8*$^{-/-}$ mice predisposes to TLR7-dependent autoimmune diseases (Demaria et al., 2010). TLR8 was similar to TLR7 in competing with TLR9 for association with Unc93B1 (Fukui et al., 2009). Given that mouse TLR8 does not deliver an activation signal, TLR8 is likely to be trafficked together with TLR7 from the ER to endolysosomes and compete there with TLR7 for RNA sensing. Thus, TLR7 activity is tightly controlled by a 2-fold antagonism in sensor transportation and nucleic acid sensing by TLR9 and TLR8, respectively.

In the steady state, self nucleic acids are considered to be kept sequestered from the endolysosome. The present study, however, demonstrated that aberrant trafficking of TLR7 and 9 was sufficient for causing systemic inflammation. A small amount of self-nucleic acids are likely to be transported to endolysosomes even in the steady state and able to stimulate TLR7 and 9 in macrophages, DCs, and nucleic acid-specific B cells. Activation of TLR7 and 9 in the steady state is supported by a recent report suggesting that Unc93B1-dependent activation of TLR7 and 9 has a role in removing autoreactive B cells (Isnardi et al., 2008). Activation of TLR7 and 9 may even have a role in regulating autoimmunity. Given that an additional copy of TLR7 gene is sufficient for predisposing to autoimmunity in Yaa mice, the steady-state activation of TLR7 can easily go beyond the safety limit. To manage a risk of TLR7 activation, its trafficking is tightly controlled by Unc93B1.

Liver failure was probably induced by hepatic microcirculatory disturbance in the course of inflammatory reactions and coagulopathy leading to local hypoxia and secondary hepatic necrosis (Kerr et al., 2003; Mochida et al., 1999). These inflammatory responses responsible for blood microcoagulate-related microcirculatory disturbances in sinusoids often developed into a systemic inflammatory response (SIRS) with a lot of cytokine production by heavily infiltrated inflammatory cells, which consists mainly of macrophages. SIRS is frequently related to fulminant liver failure, which was induced by many factors such as hepatitis virus, drugs, and autoimmune hepatitis. Histological findings of moribund *Unc93b1*$^{D34A/D34A}$ mice such as acute inflammation and multilobular necrosis and thrombocytopenia are consistent with liver damage by hepatic microcirculatory disturbance caused by cytokine storm. We could find neither bile duct destruction, distinct portal fibrosis and infiltration of lymphocytes and plasma cells, nor interface hepatitis in *Unc93b1*$^{D34A/D34A}$ mice. These are histological hallmarks of primary biliary cirrhosis or a usual type of autoimmune hepatitis, respectively. Recently, cases of acute autoimmune hepatitis have been reported (Abe et al., 2007). Interestingly, this type of autoimmune hepatitis shows fatal fulminant hepatic failure with multilobular hepatic necrosis as seen in moribund *Unc93b1*$^{D34A/D34A}$ mice (Abe et al., 2007). ANA positivity in *Unc93b1*$^{D34A/D34A}$ mice suggests that acute autoimmune hepatitis occurred and led to fulminant liver failure. However, we could not exclude the possibility of hepatic sinusoidal blood stream blockage by infiltrated cells in moribund *Unc93b1*$^{D34A/D34A}$ mice. Liver failure was reported to occur via hepatic involvement of hematologic malignancy, such as Hodgkin lymphoma, non-Hodgkin lymphoma, acute myelogenous leukemia, and chronic lymphocytic leukemia (Woolf et al., 1994). The type of infiltrating cells in sinusoids in *Unc93b1*$^{D34A/D34A}$ mice should be investigated further, for consideration of the possibility of hematopoietic malignancy. Erythrocyte phagocytosis in the moribund *Unc93b1*$^{D34A/D34A}$ mice suggested a clinical entity of hemophagocytic syndrome frequently followed by liver failure because of SIRS (Kuwata et al., 2006). Hemophagocytic syndrome is often attributed to hematopoietic malignancy (Janka, 2007).

T cells in *Unc93b1*$^{D34A/D34A}$ mice showed marked differentiation into memory phenotypes and upregulation in cell surface ICOS and CD69. Production of T cell-derived cytokines such as IL-17A, IL-21, IL-22, and IFN-γ was upregulated. IFN-γ is reported to activate macrophages and cause hemophagocytic syndrome (Jordan et al., 2004). *Unc93b1*$^{D34A/D34A}$ mice showed hemophagocytosis in the bone marrow and peripheral blood. T cell-derived cytokines such as IFN-γ are likely to contribute to monocyte activation, expansion, and infiltration in *Unc93b1*$^{D34A/D34A}$ mice.

T cell activation in *Unc93b1*$^{D34A/D34A}$ mice was dependent on B cells, as indicated by the fact that the lack of B cells completely abolished T cell activation revealed by a memory phenotype and ICOS upregulation. TLR7-dependent B cell activation is likely to lead to T cell activation and disease progression. MRL/lpr mice are similar to *Unc93b1*$^{D34A/D34A}$ mice in that the lack of B cells abolishes spontaneous T cell activation (Chan et al., 1999b). Interestingly, antibody is not required for spontaneous T cell activation in MRL/lpr mice (Chan et al., 1999a), suggesting that the antigen presenting cell (APC) function of B cells is critical in promoting diseases. Pathogenic roles for B cells are further underscored by B cell-targeted therapies that ameliorate

disease severity in several human autoimmune disorders (Dörner et al., 2009; Edwards and Cambridge, 2006).

Aberrant B cell activation in *Unc93b1*$^{D34A/D34A}$ mice is obvious from the B cell increase in number in spleen and lymph nodes and from an increase in serum IgG2a and IgG2b. B cells showed enhanced proliferation upon ligation of BCR as well as of TLR7. Considering that the basal titers of serum IgM and IgG in unperturbed *Tlr7*$^{-/-}$ mice were lower than those in wild-type mice (Demaria et al., 2010), TLR7 in B cells is likely to be constitutively activated in vivo. Given that TLR7 synergistically enhances BCR signaling (Tsukamoto et al., 2009), constitutive activation of TLR7 in *Unc93b1*$^{D34A/D34A}$ B cells would lead to strengthened BCR signaling and resultant mature B cell expansion. Decrease in marginal zone B cells in *Unc93b1*$^{D34A/D34A}$ mice is likely to be due to upregulated BCR signaling. A similar phenotype was reported in other mutant mice with strengthened BCR signaling (Pillai and Cariappa, 2009). T cell-B cell interaction activates both T and B cells, generating a vicious circle in a variety of autoimmune diseases (Edwards and Cambridge, 2006). Therefore TLR7 may have a role in maintaining or amplifying the vicious circle between T cells and B cells.

Our results, however, do not necessarily negate a role for DCs or macrophages in disease progression in *Unc93b1*$^{D34A/D34A}$ mice. In the case of MRL/lpr mice, disease progression is ameliorated not only by the lack of B cells but also by the lack of DCs (Teichmann et al., 2010). DCs are specifically required for T and B cell expansion, but not for initial T cell activation. B cells and DCs seem to have a distinct role in disease progression in MRL/lpr mice. The D34A mutation in Unc93B1 rendered TLR7 hyperresponsive in cDCs, pDCs, and macrophages as well as in B cells. DCs or macrophages may be as pathogenic as B cells in *Unc93b1*$^{D34A/D34A}$ mice. IFN-α production by pDCs has been implicated in SLE-type autoimmune diseases (Banchereau and Pascual, 2006), and pDCs showed hyperresponsiveness to TLR7 ligand in *Unc93b1*$^{D34A/D34A}$ mice. We, however, have not yet obtained evidence for pDCs activation in vivo. Furthermore, aberrant production of IP-10, a type I IFN-dependent cytokine, was not observed in the sera (data not shown). Further study is required to reveal roles for pDC, cDCs, and macrophages in T cell activation and disease progression in *Unc93b1*$^{D34A/D34A}$ mice.

In conclusion, Unc93B1 actively and continuously regulates excessive TLR7 activation of immune cells by employing TLR9 to counteract TLR7. The present study raises an important question as to what causes a shift of the TLR7 and 9 balance to TLR7 in the steady state or disease state. Future study on this issue might reveal a novel pathologic basis for inflammatory diseases in mice and humans.

EXPERIMENTAL PROCEDURES

Generation of *Unc93b1*$^{D34A/D34A}$ Mice

Targeting vector for *Unc93b1*$^{D34A/D34A}$ mice was constructed from pBAC-RP23-86M22 with Red/ET Counter-Selection BAC Modification Kit (GENE BRIDGES). The vector was designed to replace the 34th aspartic acid (GAC) to alanine (GCC). The neomycin-resistant gene was put between Loxp sequences to be deleted after germline transmission. 30 mg of targeting vector was electroporated into EB3 129/Ola strain embryonic stem cells (Niwa et al., 2000). Cells were selected with G418 and genomic DNA was purified. DNA was digested with the HindIII restriction enzyme and subjected to Southern blotting for detection of homologous recombination. The confirmed clone was microinjected into blastocysts derived from C57BL/6 mice. The obtained chimera male mice were mated with C57BL/6 female mice. Germline transmission was confirmed by coat color and heterozygous male mice were mated with female CAG-Cre transgenic mice (Sakai and Miyazaki, 1997). After neomycin-resistant gene deletion, D34A heterozygous mice were intercrossed to generate *Unc93b1*$^{D34A/D34A}$ mice. The D34A mutation in homozygous mice was confirmed by genomic DNA sequencing. All animal experiments were done with the approval of the Animal Research Committee of the Institute of Medical Science, The University of Tokyo.

Reagents and Antibodies

Recombinant murine macrophage colony-stimulating factor (M-CSF), granulocyte macrophage colony-stimulating factor (GM-CSF), and *fms*-like tyrosine kinase-3 ligand (Flt3-L) were purchased from Peprotech. Loxoribine was purchased from Alexis. Imiquimod and poly(I:C) were purchased from Invivogen. Lipid A Re:595 was purchased from SIGMA-ALDRICH. CpG-A 1585 (G*G*GGTCAACGTTGAG*G*G*G*G, asterisks are phosphorothioated) was synthesized by Hokkaido System Science. CpG-B 1668 (TCCATGACGTTCCT GATGCT, all phosphorothioated) was synthesized by FASMAC. Goat anti-IgM, F(ab′)2 fragments of affinity-purified antibodies was purchased from Jackson Immuno Research. Anti-biotin and anti-B220 MACS beads were purchased from Miltenyi Biotec. PMA and ionomycin were purchased from Calbiochem. Protein transport inhibitor was purchased from BD Biosciences PharMingen. Biotin-conjugated anti-CD11c, anti-Ter119, anti-ICOS, anti-CD69, and anti-CD21, FITC-conjugated anti-Gr1, anti-B220, and anti-CD44, PE-conjugated anti-CD11b, anti-CD71, anti-CD62L, and anti-CD23, and APC-conjugated anti-CD4 and anti-CD8 were purchased from eBioscience. FITC-conjugated anti-IFN-γ, PE-conjugated anti-CD3ε, and APC-conjugated streptavidin were purchased from BD Biosciences PharMingen. PE-conjugated anti-IL-17A was purchased from BioLegend. ELISA kit for TNF-α, IL-12p40, and IP-10 were purchased from R&D systems. ELISA kit for IFN-α was purchased from PBL interferon source. Antibodies and standard immunoglobulin for serum immunoglobulin ELISA assay was purchased from Southern Biotech.

Histological Analysis

Organs were fixed by 3.7% formaldehyde in PBS and embedded in paraffin wax for slice. Sliced organs were stained by hematoxylin and eosin (H&E) or silver impregnation and observed by BX41 microscopy system (OLYMPUS). Images were retouched with Adobe Photoshop software.

Haematological Analysis

Blood samples were obtained from mice tails with EDTA-treated vacuum capillaries and hematological scores were measured by automatic haemocytometer MEK-6450 Celltac α (Nihon Kohden).

Biochemical Test

Blood was obtained from mice inferior vena cava and separated serum was subjected to biochemical test (performed by Oriental Yeast Corporation).

Flow Cytometry

Liver, spleen, and lymph node (axillary, inguinal, and brachial) were obtained from mice and prepared to single-cell suspension. Cells were treated by NH_4Cl solution for RBCs lysis and stained with antibodies. For internal cytokine staining of T cells, cells were cultured with 50 ng/ml PMA, 1 μM ionomycin, and 4 μl/6 ml protein transport inhibitor at 37°C for 5 hr. Cells were collected and treated with heat-inactivated mouse serum at 4°C for 10 min for surface blocking. Blocked cells were stained with anti-CD4 and 7-AAD (SIGMA-ALDRICH) and fixed with 4% paraformaldehyde in PBS at 4°C overnight. Fixed cells were treated with permeabilization buffer (0.5% Triton X-100, 50 mM NaCl, 5 mM EDTA, 0.02% NaN_3 [pH 7.5]) at 4°C for 10 min and subjected to internal staining. Stained cells were subjected to flow cytometry (FACS Calibur, BD Biosciences), and acquired data were analyzed with FlowJo software (Tree Star).

Cell Culture

Culture medium for macrophages employed DMEM with 10% FCS, penicillin, and streptomycin. Culture medium for cDCs, pDCs, B cells, or T cells employed RPMI 1640 medium with 10% FCS, penicillin, and streptomycin. Indicated reagents were contained in the medium.

Deriving Myeloid Cells

Cells in bone marrow were flushed from mouse tibiae and femurs. After lysis of RBCs, cells were cultured at 37°C for 1 week. For macrophages, cDCs, or pDCs, 100 ng/ml M-CSF, 10 ng/ml GM-CSF, or 30 ng/ml Flt3-ligand were added, respectively. Cell differentiation was checked by staining CD11b or CD11c for macrophages or cDCs, respectively. For pDCs, Flt3-ligand-induced cells were stained by anti-CD11c and anti-B220. Stained cells were subjected to sorting with FACS Aria and $CD11c^{+}B220^{+}$ population was collected as pDCs.

ELISA

Production of cytokines, interferon, and serum immunoglobulin was detected by ELISA assay as described previously (Fukui et al., 2009).

Purification of B Cells

Spleens were obtained from mice and prepared to single-cell suspension. After RBC lysis, cells were stained with anti-B220 and anti-CD11c and subjected to cell sorting with FACS Aria. $B220^{+}CD11c^{-}$ cells were collected as B cells and used for analysis.

Generation of Double-Mutant Mice

Tlr7$^{-/-}$, *Tlr9*$^{-/-}$, and *Myd88*$^{-/-}$ mice were obtained from S. Akira (Osaka Univ.). *Rag2*$^{-/-}$ mice were obtained from F.W. Alt (Harvard Univ.). *Ighm* mice were purchased from The Jackson Laboratory. To obtain double-mutant mice, *Unc93b1*$^{D34A/D34A}$ mice (129 background) were crossed with genetically ablated mice (C57BL/6 background). Heterozygous mice were intercrossed to obtain double-mutant mice as well as *Unc93b1*$^{D34A/D34A}$ mice for control mice. *Unc93b1*$^{D34A/D34A}$ mice of 129 × B6 background were indistinguishable from those of 129 background in the phenotypes studied.

Intracellular Distribution of TLRs

GFP-tagged TLR7 and TLR9 were cloned into a retroviral vector pMX-puro. These genes were transfected into stem cell-derived DCs as described previously (Fukui et al., 2009). DCs were fixed and permeabilized as described in "Flow Cytometry" and stained by 5 μg/ml of Alexa-647 conjugated anti-LAMP1 for 60 min at 4°C. Cells were observed by LSM 710 confocal microscopy (Carl Zeiss) and taken images were processed by ZEN software (Carl Zeiss).

Purification of T Cells

Spleens were obtained from mice and prepared as per B cells. Cells were incubated with biotin-conjugated anti-Ter119. Anti-biotin MACS beads and anti-B220 MACS beads were bound to cells for depletion of erythroblasts and B cells. By using AutoMACS (Miltenyi Biotec), the $Ter119^{-}B220^{-}$ double-negative fraction was collected and stained with anti-CD4 and anti-CD8. CD4 single-positive or CD8 single-positive cells were sorted by FACS Aria and subjected to real-time polymerase chain reaction (PCR).

Real-Time PCR

Total RNA was purified from cells with RNeasy Kit (QIAGEN), and first-strand cDNA was synthesized with ReverTra Ace qPCR RT Kit (TOYOBO). cDNA was subjected to real-time PCR as described previously (Fukui et al., 2009). Expression of hypoxanthine guanine phosphoribosyl transferase (HPRT) mRNA in each sample was detected and used for normalization of target gene mRNA expression.

B Cell Proliferation Assay

Purified B cells were cultured with ligands for 3 days. Cell proliferation was detected by ^{3}H-labeled thymidine uptake as described previously (Tsukamoto et al., 2009), but additional culture was 5 hr.

SUPPLEMENTAL INFORMATION

Supplemental Information includes Supplemental Experimental Procedures and seven figures and can be found with this article online at doi:10.1016/j.immuni.2011.05.010.

ACKNOWLEDGMENTS

We are grateful to F. Alt and J. Miyazaki for providing mice and ES cells, to P.W. Kincade for critically reviewing the manuscript, and to T. Kitamura, T. Kaisho, and S. Takaki for their advice. We also thank K.B. Kimura for technical help for histological analyses. This work was supported (in part) by Japanese-Korean Cooperative Programme on Basic Medical Research; Grant-in-Aid for Scientific Research (B, C); Grant-in-Aid for Exploratory Research; Grant-in-Aid for Young Scientists (B and Start-up); Grant-in-Aid for Scientific Research on Innovative Areas; Joint Medical Science Research Center for the Advancement of Basic and Applied Medical Science and the Implementation of State-of-the-Art Medical Therapy; and Takeda Science Foundation.

Received: December 29, 2010
Revised: March 23, 2011
Accepted: May 18, 2011
Published online: June 16, 2011

REFERENCES

Abe, M., Onji, M., Kawai-Ninomiya, K., Michitaka, K., Matsuura, B., Hiasa, Y., and Horiike, N. (2007). Clinicopathologic features of the severe form of acute type 1 autoimmune hepatitis. Clin. Gastroenterol. Hepatol. *5*, 255–258.

Asagiri, M., Hirai, T., Kunigami, T., Kamano, S., Gober, H.J., Okamoto, K., Nishikawa, K., Latz, E., Golenbock, D.T., Aoki, K., et al. (2008). Cathepsin K-dependent toll-like receptor 9 signaling revealed in experimental arthritis. Science *319*, 624–627.

Banchereau, J., and Pascual, V. (2006). Type I interferon in systemic lupus erythematosus and other autoimmune diseases. Immunity *25*, 383–392.

Barrat, F.J., Meeker, T., Gregorio, J., Chan, J.H., Uematsu, S., Akira, S., Chang, B., Duramad, O., and Coffman, R.L. (2005). Nucleic acids of mammalian origin can act as endogenous ligands for Toll-like receptors and may promote systemic lupus erythematosus. J. Exp. Med. *202*, 1131–1139.

Barton, G.M., Kagan, J.C., and Medzhitov, R. (2006). Intracellular localization of Toll-like receptor 9 prevents recognition of self DNA but facilitates access to viral DNA. Nat. Immunol. *7*, 49–56.

Bauquet, A.T., Jin, H., Paterson, A.M., Mitsdoerffer, M., Ho, I.C., Sharpe, A.H., and Kuchroo, V.K. (2009). The costimulatory molecule ICOS regulates the expression of c-Maf and IL-21 in the development of follicular T helper cells and TH-17 cells. Nat. Immunol. *10*, 167–175.

Blasius, A.L., and Beutler, B. (2010). Intracellular toll-like receptors. Immunity *32*, 305–315.

Brinkmann, M.M., Spooner, E., Hoebe, K., Beutler, B., Ploegh, H.L., and Kim, Y.M. (2007). The interaction between the ER membrane protein UNC93B and TLR3, 7, and 9 is crucial for TLR signaling. J. Cell Biol. *177*, 265–275.

Bubier, J.A., Sproule, T.J., Foreman, O., Spolski, R., Shaffer, D.J., Morse, H.C., 3rd, Leonard, W.J., and Roopenian, D.C. (2009). A critical role for IL-21 receptor signaling in the pathogenesis of systemic lupus erythematosus in BXSB-Yaa mice. Proc. Natl. Acad. Sci. USA *106*, 1518–1523.

Casrouge, A., Zhang, S.Y., Eidenschenk, C., Jouanguy, E., Puel, A., Yang, K., Alcais, A., Picard, C., Mahfoufi, N., Nicolas, N., et al. (2006). Herpes simplex virus encephalitis in human UNC-93B deficiency. Science *314*, 308–312.

Chan, O.T., Hannum, L.G., Haberman, A.M., Madaio, M.P., and Shlomchik, M.J. (1999a). A novel mouse with B cells but lacking serum antibody reveals an antibody-independent role for B cells in murine lupus. J. Exp. Med. *189*, 1639–1648.

Chan, O.T., Madaio, M.P., and Shlomchik, M.J. (1999b). B cells are required for lupus nephritis in the polygenic, Fas-intact MRL model of systemic autoimmunity. J. Immunol. *163*, 3592–3596.

Christensen, S.R., Shupe, J., Nickerson, K., Kashgarian, M., Flavell, R.A., and Shlomchik, M.J. (2006). Toll-like receptor 7 and TLR9 dictate autoantibody specificity and have opposing inflammatory and regulatory roles in a murine model of lupus. Immunity *25*, 417–428.

Deane, J.A., Pisitkun, P., Barrett, R.S., Feigenbaum, L., Town, T., Ward, J.M., Flavell, R.A., and Bolland, S. (2007). Control of toll-like receptor 7 expression is

essential to restrict autoimmunity and dendritic cell proliferation. Immunity *27*, 801–810.

Demaria, O., Pagni, P.P., Traub, S., de Gassart, A., Branzk, N., Murphy, A.J., Valenzuela, D.M., Yancopoulos, G.D., Flavell, R.A., and Alexopoulou, L. (2010). TLR8 deficiency leads to autoimmunity in mice. J. Clin. Invest. *120*, 3651–3662.

Deng, G.M., Nilsson, I.M., Verdrengh, M., Collins, L.V., and Tarkowski, A. (1999). Intra-articularly localized bacterial DNA containing CpG motifs induces arthritis. Nat. Med. *5*, 702–705.

Diebold, S.S., Kaisho, T., Hemmi, H., Akira, S., and Reis e Sousa, C. (2004). Innate antiviral responses by means of TLR7-mediated recognition of single-stranded RNA. Science *303*, 1529–1531.

Dörner, T., Radbruch, A., and Burmester, G.R. (2009). B-cell-directed therapies for autoimmune disease. Nat. Rev. Rheumatol. *5*, 433–441.

Edwards, J.C., and Cambridge, G. (2006). B-cell targeting in rheumatoid arthritis and other autoimmune diseases. Nat. Rev. Immunol. *6*, 394–403.

Ehlers, M., Fukuyama, H., McGaha, T.L., Aderem, A., and Ravetch, J.V. (2006). TLR9/MyD88 signaling is required for class switching to pathogenic IgG2a and 2b autoantibodies in SLE. J. Exp. Med. *203*, 553–561.

Fukui, R., Saitoh, S., Matsumoto, F., Kozuka-Hata, H., Oyama, M., Tabeta, K., Beutler, B., and Miyake, K. (2009). Unc93B1 biases Toll-like receptor responses to nucleic acid in dendritic cells toward DNA- but against RNA-sensing. J. Exp. Med. *206*, 1339–1350.

Ganguly, D., Chamilos, G., Lande, R., Gregorio, J., Meller, S., Facchinetti, V., Homey, B., Barrat, F.J., Zal, T., and Gilliet, M. (2009). Self-RNA-antimicrobial peptide complexes activate human dendritic cells through TLR7 and TLR8. J. Exp. Med. *206*, 1983–1994.

Heil, F., Hemmi, H., Hochrein, H., Ampenberger, F., Kirschning, C., Akira, S., Lipford, G., Wagner, H., and Bauer, S. (2004). Species-specific recognition of single-stranded RNA via toll-like receptor 7 and 8. Science *303*, 1526–1529.

Isnardi, I., Ng, Y.S., Srdanovic, I., Motaghedi, R., Rudchenko, S., von Bernuth, H., Zhang, S.Y., Puel, A., Jouanguy, E., Picard, C., et al. (2008). IRAK-4- and MyD88-dependent pathways are essential for the removal of developing autoreactive B cells in humans. Immunity *29*, 746–757.

Janka, G.E. (2007). Hemophagocytic syndromes. Blood Rev. *21*, 245–253.

Jordan, M.B., Hildeman, D., Kappler, J., and Marrack, P. (2004). An animal model of hemophagocytic lymphohistiocytosis (HLH): CD8+ T cells and interferon gamma are essential for the disorder. Blood *104*, 735–743.

Kaisho, T., and Akira, S. (2006). Toll-like receptor function and signaling. J. Allergy Clin. Immunol. *117*, 979–987, quiz 988.

Kerr, R., Newsome, P., Germain, L., Thomson, E., Dawson, P., Stirling, D., and Ludlam, C.A. (2003). Effects of acute liver injury on blood coagulation. J. Thromb. Haemost. *1*, 754–759.

Kim, Y.M., Brinkmann, M.M., Paquet, M.E., and Ploegh, H.L. (2008). UNC93B1 delivers nucleotide-sensing toll-like receptors to endolysosomes. Nature *452*, 234–238.

Kitamura, D., Roes, J., Kühn, R., and Rajewsky, K. (1991). A B cell-deficient mouse by targeted disruption of the membrane exon of the immunoglobulin mu chain gene. Nature *350*, 423–426.

Krieg, A.M. (2002). CpG motifs in bacterial DNA and their immune effects. Annu. Rev. Immunol. *20*, 709–760.

Kuwata, K., Yamada, S., Kinuwaki, E., Naito, M., and Mitsuya, H. (2006). Peripheral hemophagocytosis: An early indicator of advanced systemic inflammatory response syndrome/hemophagocytic syndrome. Shock *25*, 344–350.

Lande, R., Gregorio, J., Facchinetti, V., Chatterjee, B., Wang, Y.H., Homey, B., Cao, W., Wang, Y.H., Su, B., Nestle, F.O., et al. (2007). Plasmacytoid dendritic cells sense self-DNA coupled with antimicrobial peptide. Nature *449*, 564–569.

Leadbetter, E.A., Rifkin, I.R., Hohlbaum, A.M., Beaudette, B.C., Shlomchik, M.J., and Marshak-Rothstein, A. (2002). Chromatin-IgG complexes activate B cells by dual engagement of IgM and Toll-like receptors. Nature *416*, 603–607.

Marshak-Rothstein, A., and Rifkin, I.R. (2007). Immunologically active autoantigens: the role of toll-like receptors in the development of chronic inflammatory disease. Annu. Rev. Immunol. *25*, 419–441.

Miyake, K. (2007). Innate immune sensing of pathogens and danger signals by cell surface Toll-like receptors. Semin. Immunol. *19*, 3–10.

Mochida, S., Arai, M., Ohno, A., Yamanobe, F., Ishikawa, K., Matsui, A., Maruyama, I., Kato, H., and Fujiwara, K. (1999). Deranged blood coagulation equilibrium as a factor of massive liver necrosis following endotoxin administration in partially hepatectomized rats. Hepatology *29*, 1532–1540.

Nickerson, K.M., Christensen, S.R., Shupe, J., Kashgarian, M., Kim, D., Elkon, K., and Shlomchik, M.J. (2010). TLR9 regulates TLR7- and MyD88-dependent autoantibody production and disease in a murine model of lupus. J. Immunol. *184*, 1840–1848.

Niwa, H., Miyazaki, J., and Smith, A.G. (2000). Quantitative expression of Oct-3/4 defines differentiation, dedifferentiation or self-renewal of ES cells. Nat. Genet. *24*, 372–376.

Pillai, S., and Cariappa, A. (2009). The follicular versus marginal zone B lymphocyte cell fate decision. Nat. Rev. Immunol. *9*, 767–777.

Pisitkun, P., Deane, J.A., Difilippantonio, M.J., Tarasenko, T., Satterthwaite, A.B., and Bolland, S. (2006). Autoreactive B cell responses to RNA-related antigens due to TLR7 gene duplication. Science *312*, 1669–1672.

Rajagopal, D., Paturel, C., Morel, Y., Uematsu, S., Akira, S., and Diebold, S.S. (2010). Plasmacytoid dendritic cell-derived type I interferon is crucial for the adjuvant activity of Toll-like receptor 7 agonists. Blood *115*, 1949–1957.

Ronaghy, A., Prakken, B.J., Takabayashi, K., Firestein, G.S., Boyle, D., Zvailfler, N.J., Roord, S.T., Albani, S., Carson, D.A., and Raz, E. (2002). Immunostimulatory DNA sequences influence the course of adjuvant arthritis. J. Immunol. *168*, 51–56.

Sakai, K., and Miyazaki, J. (1997). A transgenic mouse line that retains Cre recombinase activity in mature oocytes irrespective of the cre transgene transmission. Biochem. Biophys. Res. Commun. *237*, 318–324.

Subramanian, S., Tus, K., Li, Q.Z., Wang, A., Tian, X.H., Zhou, J., Liang, C., Bartov, G., McDaniel, L.D., Zhou, X.J., et al. (2006). A Tlr7 translocation accelerates systemic autoimmunity in murine lupus. Proc. Natl. Acad. Sci. USA *103*, 9970–9975.

Tabeta, K., Hoebe, K., Janssen, E.M., Du, X., Georgel, P., Crozat, K., Mudd, S., Mann, N., Sovath, S., Goode, J., et al. (2006). The Unc93b1 mutation 3d disrupts exogenous antigen presentation and signaling via Toll-like receptors 3, 7 and 9. Nat. Immunol. *7*, 156–164.

Teichmann, L.L., Ols, M.L., Kashgarian, M., Reizis, B., Kaplan, D.H., and Shlomchik, M.J. (2010). Dendritic cells in lupus are not required for activation of T and B cells but promote their expansion, resulting in tissue damage. Immunity *33*, 967–978.

Tsukamoto, Y., Nagai, Y., Kariyone, A., Shibata, T., Kaisho, T., Akira, S., Miyake, K., and Takatsu, K. (2009). Toll-like receptor 7 cooperates with IL-4 in activated B cells through antigen receptor or CD38 and induces class switch recombination and IgG1 production. Mol. Immunol. *46*, 1278–1288.

van der Fits, L., Mourits, S., Voerman, J.S., Kant, M., Boon, L., Laman, J.D., Cornelissen, F., Mus, A.M., Florencia, E., Prens, E.P., and Lubberts, E. (2009). Imiquimod-induced psoriasis-like skin inflammation in mice is mediated via the IL-23/IL-17 axis. J. Immunol. *182*, 5836–5845.

Woolf, G.M., Petrovic, L.M., Rojter, S.E., Villamil, F.G., Makowka, L., Podesta, L.G., Sher, L.S., Memsic, L., and Vierling, J.M. (1994). Acute liver failure due to lymphoma. A diagnostic concern when considering liver transplantation. Dig. Dis. Sci. *39*, 1351–1358.

Yu, P., Wellmann, U., Kunder, S., Quintanilla-Martinez, L., Jennen, L., Dear, N., Amann, K., Bauer, S., Winkler, T.H., and Wagner, H. (2006). Toll-like receptor 9-independent aggravation of glomerulonephritis in a novel model of SLE. Int. Immunol. *18*, 1211–1219.

Yu, C.F., Peng, W.M., Oldenburg, J., Hoch, J., Bieber, T., Limmer, A., Hartmann, G., Barchet, W., Eis-Hübinger, A.M., and Novak, N. (2010). Human plasmacytoid dendritic cells support Th17 cell effector function in response to TLR7 ligation. J. Immunol. *184*, 1159–1167.